Desalination and Water Treatment
www.deswater.com

doi:10.5004/dwt.2017.20834

79 (2017) 19–29
June

Modification strategy of biodegradable poly (butylene succinate) (PBS) membrane by introducing Al_2O_3 nanoparticles: preparation, characterization and wastewater treatment

Melika Ebrahimpour[a], Ali Akbar Safekordi[a,*], Seyed Mahmoud Mousavi[b], Amir Heydarinasab[a]

[a]*Department of Chemical Engineering, Science and Research Branch, Islamic Azad University, Tehran, Iran, email: melika_ebrahimpour2001@yahoo.com (M. Ebrahimpour), safekordi@sharif.edu (A.A. Safekordi), email: a.heidarinasab@srbiau.ac.ir (A. Heydarinasab)*
[b]*Department of Chemical Engineering, Faculty of Engineering, Ferdowsi University of Mashhad, Mashhad, Iran, email: mmousavi@um.ac.ir (S.M. Mousavi)*

Received 18 October 2016; Accepted 16 April 2017

ABSTRACT

Novel biodegradable poly (butylene succinate) membranes were modified by introducing Al_2O_3 nanoparticles. A series of non-solvents (i.e. methanol, methanol/isopropanol (50/50, v/v), isopropanol) is used as coagulants. The correlation between membrane morphology, mechanical properties, hydrophilicity, thermal stability and permeation properties of membranes were examined as functions of non-solvents used in coagulation bath and Al_2O_3 nanoparticle concentrations. The modified membranes were characterized by contact angle, scanning electron microscopy, thermogravimetric analysis, tensile testing and dynamic test of tomato canning wastewater treatment. The experimental results elucidated that modified membranes exhibit significant differences in surface properties and inherent properties due to Al_2O_3 nanoparticles addition. In addition, a substantial increase in mechanical properties and resistance of membranes was observed for the poly (butylene succinate) membranes cast in isopropanol coagulation bath of increasing Al_2O_3 nanoparticles up to 1 wt.%. These membranes have more comprehensive potential to reject the wastewater pollutants properly than others.

Keywords: Poly (butylene succinate); Al_2O_3 nanoparticles; Membrane; Hydrophilicity; Biodegradable

1. Introduction

Biodegradable polymers have received much more attention in the last two decades due to their potential applications in the fields related to environmental protection and the maintenance of physical health [1]. Aliphatic polyesters are among the most promising materials to be considered as high performance environmentally friendly biodegradable plastics [2]. As one of the commercial and most representative biodegradable aliphatic polyesters, PBS has good degradability and melt process ability. However, other properties of PBS, such as softness, tensile and gas barrier properties, melt viscosity for further processing, etc., are frequently insufficient for various end-use applications [3]. Therefore, efforts have focused on increasing the properties of PBS either by chemical or physical modifications. These modifications of PBS have been reported in the literature [4–11]. These modifications can be divided into three categories i.e. blending polymer with hydrophilic nanoparticles such as SiO_2, ZrO_2 and TiO_2, grafting with hydrophilic polymers, monomers or functional groups and coating with hydrophilic polymers [12]. Recently, the utility of inorganic nanoparticles as additives to enhance the polymer performance has been established [13]. Blending with nanoparticles has attracted much interest in the past 10 years due to their convenient operation and mild conditions. Great efforts have been made to preparing compos-

*Corresponding author.

ites [14,15], nanocomposites [16,17], microcapsules [18] of PBS biodegradable polymer and its application is limited in field of medicine and membrane science. Recently synthetic membranes have become the focus of separation processes in different industries. Synthetic membranes may be composed of inorganic materials (like ceramics) and organic materials (like polymers). Current research on membranes mostly focus on polymeric membranes due to better control of the pore forming mechanism, higher flexibility, smaller spaces required for installation and lower costs compared to inorganic membranes [19]. Different types of membrane are made by biodegradable polymers [20–24] have become available for membrane separation processes. Since, a few studies have been conducted on PBS membranes. Ghaffarian et al. recently investigated the preparation, characterization and properties of biodegradable blend membranes of PBS/CA [3] and PES/PBS [25]. Studies of PBS-blending modifications have focused on blending the polymer with hydrophilic polymers.

Blending with inorganic nanoparticles among the aforementioned methods offers the advantage of being able to prepare artificial membranes with excellent separation performance, good thermal and chemical resistance and adaptability to the harsh wastewater environments [26]. More over the addition of inorganic nanoparticles has resulted to increased membrane permeability and improved control of membrane surface properties.

World water demand has become increasingly urgent worldwide, due to a fast growing global population and increasing water demand. The reuse of treated wastewater effluent has become a reality and many industries use this water in their production processes [12]. The tomato canning industry is one of the food industries, which produce large amount of wastewater per year. Tomato canning industry has two major types of waste streams: wastewater and solid water. High wastewaters in BOD are generated by unloading, washing and peeling processes, partly because water-soluble sugars are dissolved from the fruit. The wash water also contains suspended and dissolved organic matter. So, it is necessary to find an alternative to treat and possibly reuse tomato canning industry wastewater.

The novelty in this research lies in introducing Al_2O_3 nanoparticles to PBS in order to improve the performance of PBS membrane for tomato canning wastewater filtration. This investigation describes the preparation of pure PBS membranes and novel PBS/Al_2O_3 nanoparticles composite membranes using the phase inversion method by including different Al_2O_3 nanoparticle concentrations to the casting solution. The effects of non-solvent used in the coagulation bath and Al_2O_3 nanoparticle concentration on morphology, mechanical properties, thermal behavior, hydrophilicity and permeation flux of the PBS membranes were investigated.

2. Experimental

2.1. Material

Poly (butylene succinate) (d: 1.3 g/ml at 25°C) extended with 1,6-diisocyanatohexane and Al_2O_3 nanoparticles (<50 nm in size) were purchased from Sigma-Aldrich. PBS was dried in vacuum oven at 60°C for 6 h before use. Analytical grade and high purity 1,1,2,2-tetrachloroethane was supplied from SAMCHUN (Korea) and was used as the solvent. Methanol with a purity of 99.8 wt.% from QRec, isopropanol with a purity of 96 wt.% from Merck were used without further purification as non-solvents. All experiments were performed at a constant temperature of 25°C. Wastewater sourced for this research was provided from a local tomato paste factory. Three pollution indices of the wastewater i.e. turbidity, chemical oxygen demand (COD) and total dissolved solids (TDS) were in the value of 286 NTU, 1473 mg/l, and 1207 mg/l, respectively.

2.2. Membrane preparation

Fig. 1 shows the shear viscosity of PBS/1,1,2,2-Tetrachloroethane solutions as a function of polymer concentration at a shear rate 12 s^{-1}. The two linear portions of the viscosity curve are extrapolated and the polymer concentration are corresponding to the intersection point of the two lines is defined as the critical value of concentration. Based on Fig. 1, the critical polymer concentration is about 16 wt.%. In the viscosity greater than the critical value, the polymer exhibits significant chain entanglement [27], which aids the formation of dense skin with minimal defects on the membrane performance.

Poly (butylene succinate) (PBS) asymmetric membranes were fabricated via phase inversion induced by immersion precipitation [28]. Before the preparation of casting solution, the Al_2O_3 nanoparticles are needed to be prepared. If they are added to the casting solution untreated, the inorganic nanoparticles would aggregate and the modified membranes would not have been as effective. So, to increase their dispersibility in the casting solution, the inorganic nanoparticles should be treated. For this purpose 5.0 g of Al_2O_3 was added to a 1000 ml 3.5% SDS solution and the solution pH was adjusted to 4. After 8 h of vigorous stirring, the solution was centrifuged and vacuum filtered so as to isolate the inorganic nanoparticles [29]. The isolated nanoparticles then were vacuum dried for 6 h at 50°C to remove any remaining water. After drying, the particles were ready for adding to the casting solution. In phase inversion induced by immersion precipitation the polymer solution is immersed in a non-solvent coagulation bath. Demixing and precipitation occur due to the exchange

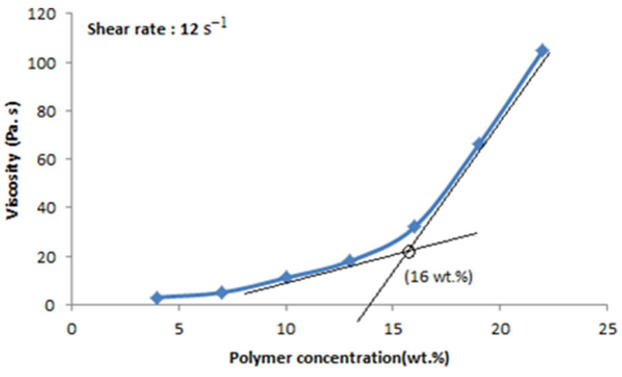

Fig. 1. Critical concentration of PBS/1,1,2,2-Tetrachloroethane dope solution.

of solvent (from polymer solution) and non-solvent (from coagulation bath), that is the solvent and non-solvent must be miscible [30]. For modified PBS membrane preparation firstly Al_2O_3 nanoparticles (0.5, 1, 1.5 and 2 wt.%, respectively), dispersing in the 1,1,2,2-Tetrachloroethane as a solvent. Then this solution is sonicated for 48 h at approximately 25°C to obtain a uniform and homogeneous casting suspension. The PBS (16 wt.%) was added to the each of Al_2O_3 nanoparticle solution and the mixture was further sonicated for 3 d until a homogeneous solution was formed. After degassing, an appropriate amount of this suspension was cast with 250 µm casting knife onto a glass plate. The nascent membrane was evaporated at ambient temperature for 30 s and then immersed in methanol, isopropanol and methanol/isopropanol (50/50, v/v) coagulation bath. For all prepared membranes, after completing coagulation, the membranes were transferred to ultra-pure water for 6 h at ambient temperature to remove the remaining solvent from the membrane structure before testing.

2.3. Determination of cloud point value and phase diagram

A phase diagram can predict whether or not a solution of a certain polymer in a certain solvent is suitable for membrane formation. Ternary phase diagram is useful for the prediction of the phase transitions that cloud occur when phase separation is induced according to immersion precipitation method [31]. The phase diagram of the PBS/solvent / non-solvent combination system was determined by cloud point measurement. Hence, cloud point data were obtained by the titration method. The ternary phase diagram (cloud points curve) was obtained by the following method: PBS solution with different composition was taken into a glassware under stirring and the non-solvent was slowly added to the PBS solution from a burette until the clear polymer solution visually turned to cloudy. The ternary composition of cloud point was then calculated from the weight of non-solvent, solvent and polymer present in the glass-ware. All the experiments were carried out at ambient temperature (25°C).

2.4. Membrane characterization

2.4.1. Scanning electron microscopy (SEM)

Scanning electron microscopy (SEM) was used to study the morphology of membranes. SEM images were made with a KYKY EM3200 instrument with an accelerating voltage of 25 kV. Top surface and cross-section images were prepared by fracturing the dried membranes in liquid nitrogen. The membranes were then coated with a thin film of gold to minimize sample charging problems.

2.4.2. Contact angle measurements

The contact angle measurements are measured to evaluate surface hydrophilicity of the membranes impregnated with Al_2O_3 nanoparticles and neat membranes using a contact angle measuring instrument [G10, KRUSS, Germany]. For this purpose a water droplet was deposited on a membrane surface and the contact angle between the water and membrane was measured until no further change was observed. The average contact angle for deionized water was determined in a series of three measurements for each different membrane surfaces.

2.4.3. Thermogravimetric analysis (TGA)

Decomposition characteristics and thermal stability of the samples were determined by Thermogravimetric analysis (TGA) using TGA-50 (Shimudza company, Japan). About 5 mg of each sample was placed in the ceramic pan and heated in the temperature range of 25–800°C at a rate of 10°C/min under nitrogen atmosphere.

2.4.4. Mechanical evaluation

Tensile testing to study tensile strength, tensile modulus and elongation at break (%) were performed using SANTAM 20KN testing machine at 25°C (ambient temperature). All tests were done according to ASTM D638 standard and were carried out with a crosshead speed of 10 mm/min. The film specimens had a dimension of 70 × 10 × 0.25 mm. The grip distance was 50 mm and the gage length was 25 mm. Property reported values here represent an average of the results for tests run on three specimens.

2.4.5. Permeation experiments

The new synthetic membranes were characterized for pure water permeability and solute rejection analyzing using a batch cross-flow filtration set-up with an effective filtration area of 50.24 cm^2 (Fig. 2). The obtained membrane samples were cut into circle membrane species of 6 cm in diameter and set in membrane module of a laboratory scale filtration apparatus. The measuring procedure was described as follows: at first, to alleviate the impact of compaction on flux, pre-filtration studies with pure deionized water (DIW) were conducted until a steady state flux was achieved. Thus, transmembrane pressure (TMP) is increased gradually to 7 bar and membranes were initially compacted at this pressure at 25°C to get a steady flux. Then the flux was recorded every 10 min, at least 5 readings were collected to obtain an average value. For tomato canning wastewater filtration, the transmembrane pressure was kept constant at 7 bar and permeate flux was determined by monitoring the volume of permeate with time. Permeate flux was obtained from the volume of the permeate within 60 and 30 min for pure water, tomato canning wastewater respectively and calculated as [32]:

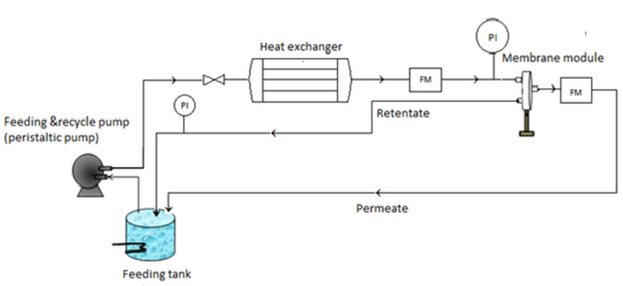

Fig. 2. Schematic diagram of the experimental setup.

$$J = \frac{Q}{A \times t} \quad (1)$$

where J is the permeation flux (L/m²h), Q is the permeate volume (L), A is the membrane area (m²) and t is the time (h).

Solute rejection was measured at 7 bar and calculated by Eq. (2) [33]:

$$R(\%) = \left(1 - \frac{C_p}{C_f}\right) \times 100\% \quad (2)$$

where C_p and C_f are the concentration of pollution indices in permeate and feed respectively.

Membrane hydraulic resistance (R_m) is the intrinsic resistance of the membrane determined using pure water as feed at different transmembrane pressures of (2 to 7 bars) and obtained by Eq. (3) [34].

$$R_m = \frac{\Delta P}{\mu j_w} \quad (3)$$

where ΔP, μ and j_w are transmembrane pressure (Pa), viscosity of permeate (Pa·s) and permeation flux (m³/m²·s), respectively.

Because the viscosity varies with temperature, it has to be measured throughout the experiment. In the case of water, the viscosity can be calculated using the following equation [35]:

$$\mu(T) = 1.73\exp(-0.0268T) \quad (4)$$

where T is the temperature (°C). This equation is valid for 0°C < T < 30°C.

Finally, each membrane filtrate would be analyzed for different pollution indices of turbidity, total dissolved solids (TDS) and chemical oxygen demand (COD).

3. Results and discussion

3.1. Phase diagram of PBS/1,1,2,2-Tetrachloroethane/non-solvent system

Ternary phase diagrams are useful for the prediction of the phase transitions that could occur when phase separation is induced according to immersion precipitation method [31]. Thermodynamic analysis reveals the effect of interaction potentials on the mixing and demixing of blended components, which are often demonstrated by phase diagrams [27]. The phase diagrams for the system PBS/1,1, 2,2-Tetrachloroethane/non-solvent represents a detailed picture of the three components miscibility and it contains useful thermodynamic information about the phase inversion process. The ternary phase diagram of the PBS/ 1,1,2,2-Tetrachloroethane/ non-solvent combination systems are obtained from the cloud points measurements which are presented in Fig. 3. As shown, the gelation boundary for the PBS/1,1,2,2-Tetrachloroethane/methanol system is closer to the polymer–solvent axis as compared to the other PBS/1,1,2,2-Tetrachloroethan/ non-solvent systems. Hence, according to Fig. 3, the coagulation power of the coagulants is in the order of: methanol > methanol/isopropanol (50/50, v/v) > isopropanol. Therefore, only a small amount of methanol is needed to disturb the solution system equilibrium and induce the polymer precipitation. The results suggest that the thermodynamic stability of the PBS/1,1,2,2-Tetrachloroethane/non-solvent systems follows the sequence: methanol < methanol/isopropanol (50/50, v/v) < isopropanol.

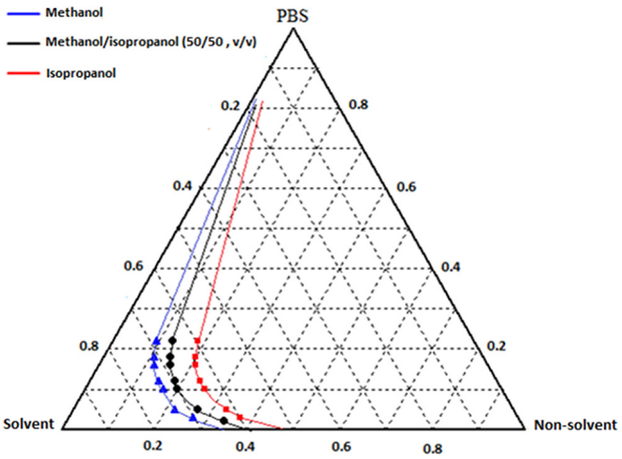

Fig. 3. Ternary phase diagram of PBS/solvent/non-solvent system.

3.2. Morphology of membranes

3.2.1 The effect of Al_2O_3 nanoparticles concentration

SEM analysis provides a visual and quantitative characterization of the surface and cross sectional morphology of unmodified and modified membranes coagulated in methanol, isopropanol and methanol/isopropanol (50/50, v/v) coagulation mediums . Figs. 4–7 show the SEM images of

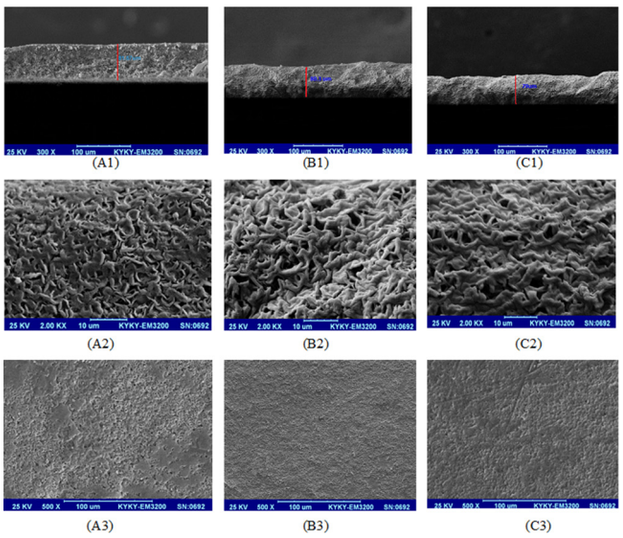

Fig. 4. SEM images of the neat PBS membrane that is prepared in different coagulation baths: (A1), (A2): cross section and (A3): top surface of neat PBS membrane, non-solvent: methanol, (B1), (B2): cross section and (B3): top surface of neat PBS membrane, non-solvent: methanol/isopropanol (50/50, v/v) and (C1), (C2): cross section and (C3): top surface of neat PBS membrane, non-solvent: isopropanol.

the surface, cross section structure of the membranes. As can be seen in the images, in the neat membranes fabricated

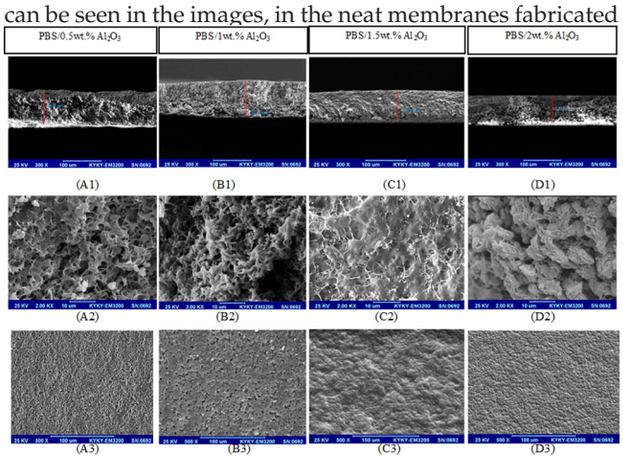

Fig. 5. SEM images of the PBS/Al_2O_3 membranes prepared in methanol coagulation bath at different concentrations of Al_2O_3 nanoparticle: (A1), (A2): cross section and (A3): top surface of PBS/0.5 wt.% Al_2O_3, (B1), (B2): cross section and (B3): top surface of PBS/1 wt.% Al_2O_3, (C1), (C2): cross section and (C3): top surface of PBS/1.5 wt.% Al_2O_3 and (D1), (D2): cross section and (D3): top surface of PBS/2 wt.% Al_2O_3.

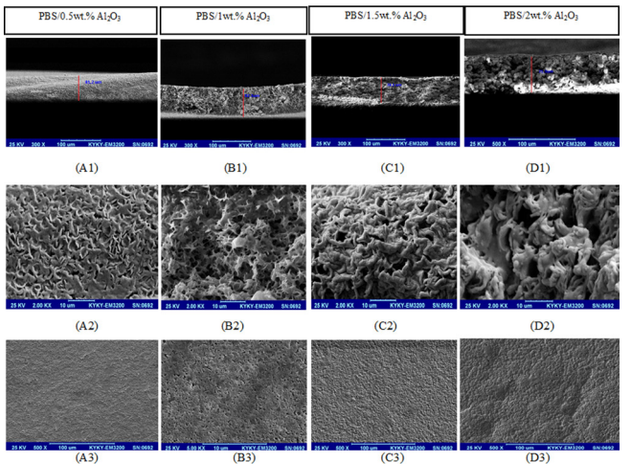

Fig. 6. SEM images of the PBS/Al_2O_3 membranes prepared in methanol/isopropanol (50/50, v/v) coagulation bath at different concentrations of Al_2O_3 nanoparticle: (A1), (A2):cross section and (A3): top surface of PBS/0.5 wt.% Al_2O_3, (B1), (B2): cross section and (B3): top surface of PBS/1 wt.% Al_2O_3, (C1), (C2): cross section and (C3): top surface of PBS/1.5 wt.% Al_2O_3 and (D1), (D2): cross section and (D3): top surface of PBS/2 wt.% Al_2O_3.

by PBS a dense thin top layer was formed, and a sponge-like structure was observed in the sublayer of resulting membranes. Also, all membranes exhibit an asymmetric structure and there is no significant difference between the modified and unmodified membrane's structure. However, it is also clear that the Al_2O_3 nanoparticles significantly affected on the porosity of the PBS membranes. The presence of affinity and interaction between Al_2O_3 nanoparticles and coagulant provides a great permeation velocity of coagulant into nascent membrane during the phase inversion. Moreover, solvent diffusion from the membrane to the

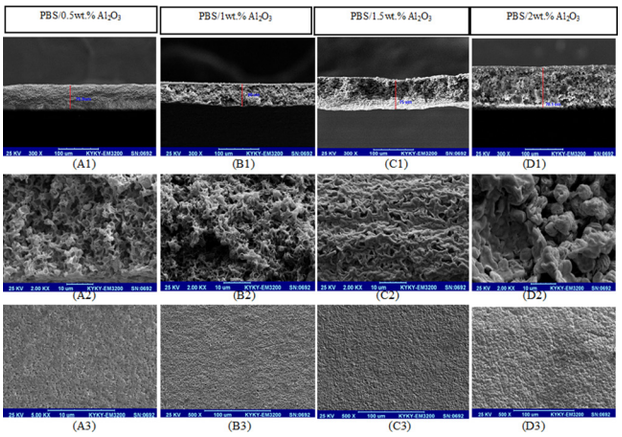

Fig. 7. SEM images of the PBS/Al_2O_3 membranes prepared in isopropanol coagulation bath at different concentrations of Al_2O_3 nanoparticle: (A1), (A2): cross section and (A3): top surface of PBS/0.5 wt.% Al_2O_3, (B1), (B2): cross section and (B3): top surface of PBS/1wt.% Al_2O_3, (C1), (C2): cross section and (C3): top surface of PBS/1.5 wt.% Al_2O_3 and (D1), (D2): cross section and (D3): top surface of PBS/2 wt.% Al_2O_3.

coagulant can also be increased by the addition of Al_2O_3 nanoparticles. In presence of Al_2O_3 nanoparticles the interaction between polymer and solvent molecules decreases, so solvent molecules can diffuse more easily from the polymer matrix in to coagulant [36]. Thus, pore size and porosity of impregnated membrane with Al_2O_3 nanoparticles can be higher than the neat PBS membrane. It's clear that an increase with higher concentration of Al_2O_3 nanoparticles (up to 1.5 wt.%), significant agglomeration takes place. In terms of both performance and economy, 1 wt.% of Al_2O_3 nanoparticles in the casting solution were found to be ideal.

3.2.2. *The effect of non-solvent used in coagulation bath*

All prepared membranes in three different non-solvents as coagulation baths i.e. methanol, methanol/isopropanol (50/50, v/v) and isopropanol are observed to be porous and asymmetric with sponge-like structures. Significant finding is that the porosity is slightly decreased when the coagulant component is changed from methanol to methanol/isopropanol (50/50, v/v) and isopropanol as respectively shown in Figs. 4–7. Due to the large polar parameter (δ_p) of methanol as non-solvent, which indicates its high polarity, it can be predicted that this alcohol has appropriate interaction with the polar section of PBS polymer. In addition to this property, the small size of methanol compared with isopropanol (particularly methanol small size) makes a great tendency and ability for penetration in to nascent film in coagulation bath and the exchange process of solvent/non-solvent can be accelerated. Thus, more porous structure of membrane is obtained. Generally, a higher diffusion of a non-solvent (methanol) in a solvent (1,1,2,2- tetrachloroethane) results in a faster precipitation [27], that may induce delayed solid-liquid demixing during the formation of membrane. Therefore, the liquid–liquid demixing controls the phase separation. However, by introducing isopropanol as non-solvent, the liquid–liquid demixing process is

delayed and the solid–liquid demixing process occurs. With increasing isopropanol content in the coagulation bath, the phase separation process is eventually dominated by the solid–liquid demixing. These observations are in agreement with the phase diagram (Fig. 3).

From ternary diagram that can be found methanol has the strongest coagulation power than others. Since its cloud point curve is closer to the PBS-solvent axis on the triangular diagram. The difference in Hansen's solubility parameters between PBS and the non-solvents is of the order (PBS-methanol) > (PBS-methanol/isopropanol (50/50, v/v)) > (PBS-isopropanol). A larger difference in solubility parameter with polymer usually implies a shorter time for solid–liquid demixing process to occur.

3.3. Mechanical properties of membranes

Fig. 8 shows the mechanical properties of the membranes. Generally, it's found that all mechanical properties of the modified membranes are improved compared to the neat PBS membranes. In general, the tensile strength and young's modulus are increased with incorporation of Al_2O_3 nanoparticles in the membranes. As can be seen, incorporation of 1 wt.% Al_2O_3 nanoparticles enhanced the tensile strength of membranes prepared in isopropanol coagulation bath by about 26% compared to its counterpart without any nanoparticle additives. Also, significant improvement in the young's modulus of membranes prepared in isopropanol (26%) was obtained by the incorporation of 1 wt.% Al_2O_3 nanoparticles. This might be explained by the fact that the higher ratio surface area and activity of Al_2O_3 nanoparticles filled in the polymer chains cause self-relative conglutination force in the membrane structure. Also the free motion of polymeric chains is partly restricted by the intermolecular forces between the polymeric chains and the inorganic oxide nanoparticles dispersed uniformly in polymer. So the tensile strength of membranes is sequentially enhanced [37]. Afterwards, the break resistance of membranes is improved and the mechanical properties are enhanced. However, excessive amount of Al_2O_3 nanoparticles more than a certain concentration of 1 wt.% is leading to insignificant increase in the membrane's tensile strength as the Al_2O_3 nanoparticles coalesces. Elongation-at-break of

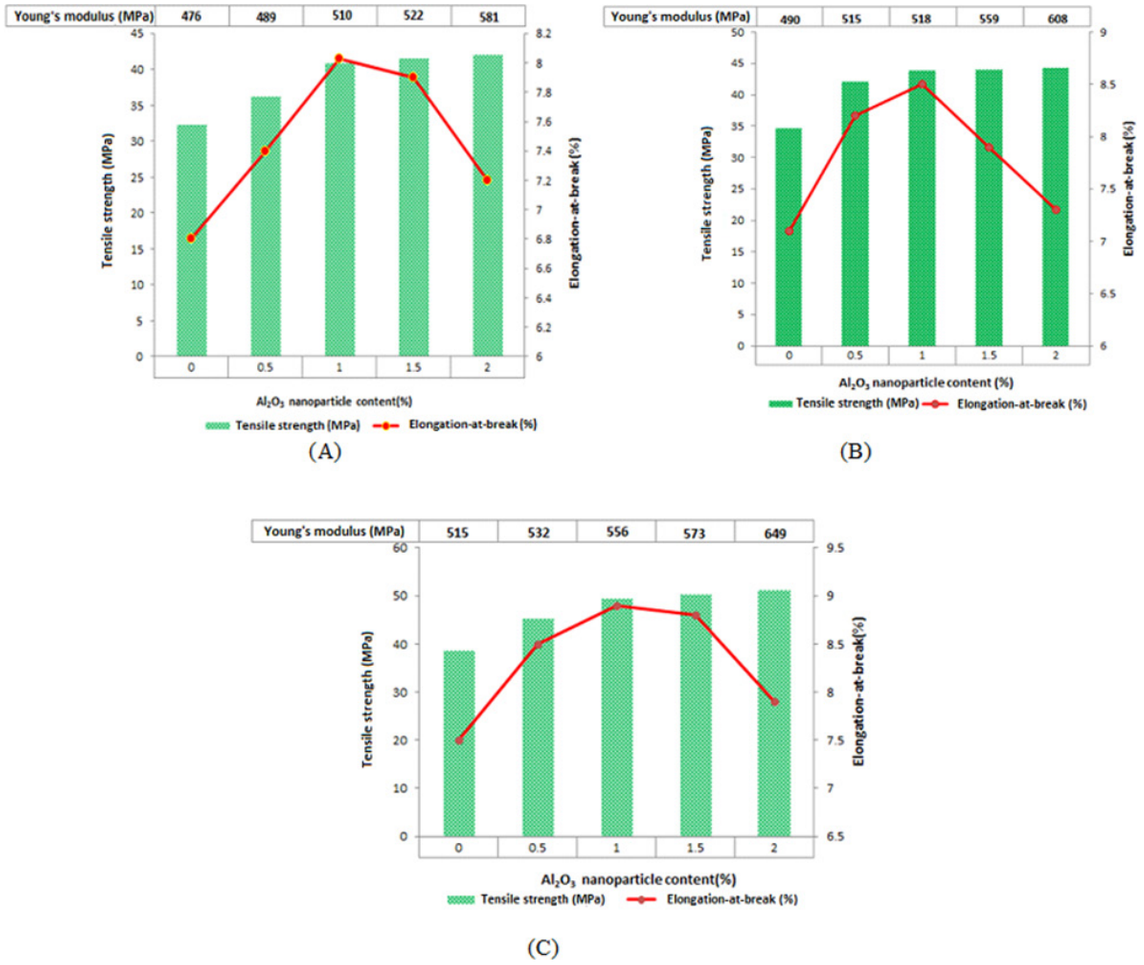

Fig. 8. Mechanical properties of the membranes A) membrane prepared in methanol coagulation bath, B) membrane prepared in methanol/isopropanol, 50/50 (v/v) coagulation bath, C) membrane prepared in isopropanol coagulation bath.

membranes prepared at three different coagulation bath increased with increasing Al_2O_3 nanoparticles content to 1 wt.% and then decreased when Al_2O_3 nanoparticles content reached to 2 wt.% . In fact, adding an excessive amount of Al_2O_3 nanoparticles (more than 1 wt.%) causes the membrane elasticity to decline slightly. This behavior is definitely due to the brittleness of Al_2O_3 nanoparticles in comparison with the flexibility of polymer chains. Regarding section 3.2., the membranes prepared at methanol coagulation bath are more porous. The high porosity and large cavities in the membrane structure decrease the mechanical properties [38] so the membranes were prepared in methanol coagulation bath have relatively poor mechanical properties due to more porosity than others. In particular, the membranes containing 1 wt.% of Al_2O_3 nanoparticles prepared in isopropanol coagulation bath showed the highest young's modulus about 556 MPa that was much higher than that of prepared at methanol coagulation bath (510 MPa) .

3.4. Thermal stability of membranes

The prepared membranes in methanol coagulation bath are evaluated by TGA thermograms. The typical TGA thermograms are shown in Fig. 9 and the degradation data are summarized in Table 1. The peak degradation temperature (T_{max}) of 368.7°C is exhibited for neat PBS membrane and is increased to 423.3°C for the modified membrane (PBS/1 wt.% Al_2O_3 nanoparticles). The onset degradation temperatures (T_{onset}) for PBS/(0 wt.% Al_2O_3 nanoparticles), PBS/(1 wt.% Al_2O_3 nanoparticles) are 314.06 and 378°C, respectively. Similarly, the end of degradation temperatures (T_{end}) for these membranes is at 418 and 478°C, respectively. The modified membrane shows higher thermal stability than that of neat PBS membrane. This might be explained by the fact that inorganic nanoparticles absorb heat, and therefore the membranes' thermal properties should improve [39]. On the other hand, inherent high thermal stability of Al_2O_3 nanoparticles may result an improvement in heat resistance of polymer matrix. As can be on thermograms thermal stability of PBS membrane is improved by an increase of 60°C after modified membrane preparation with Al_2O_3 nanoparticles.

3.5. Contact angle measurement

The contact angle is an important parameter for measuring surface hydrophilicity [40]. Generally, a small contact angle indicates greater hydrophilicity whereas a large contact angle indicates greater hydrophobicity. PBS is a hydrophobic polymer. Its hydrophilicity can be improved significantly by the addition of Al_2O_3 nanoparticles, which have some desired characteristics, such as hydrophilicity and higher ratio surface areas. Fig. 10 illustrates the results of this analysis. As shown in Fig. 10, addition of Al_2O_3 nanoparticles from 0 wt.% to 1 wt.% gently improves the final membrane surface porosity. As a result, the values of contact angle for these membranes have descending trend. The membranes were prepared in methanol coagulation bath have relatively low contact angles due to more porosity than others.

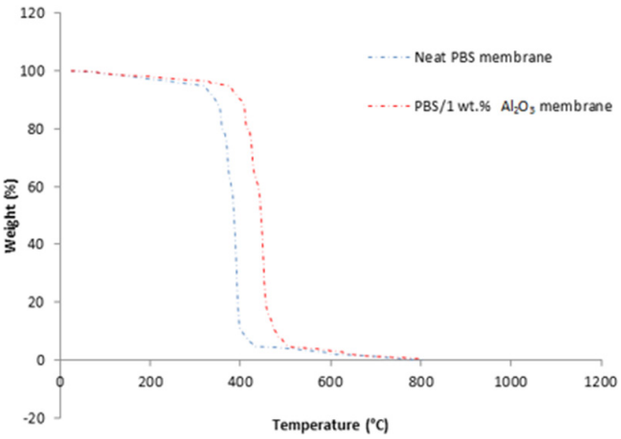

Fig. 9. TGA curves of the neat and modified PBS membranes.

Table 1
Thermal Properties of neat PBS and PBS/1 wt.% Al_2O_3 membranes determined by TGA thermograms

Sample	T_{onset} (°C)	T_{max} (°C)	T_{end} (°C)
PBS/(0 wt.% Al_2O_3)	314.06	368.77	418.4
PBS/(1 wt.% Al_2O_3)	378	423.3	478

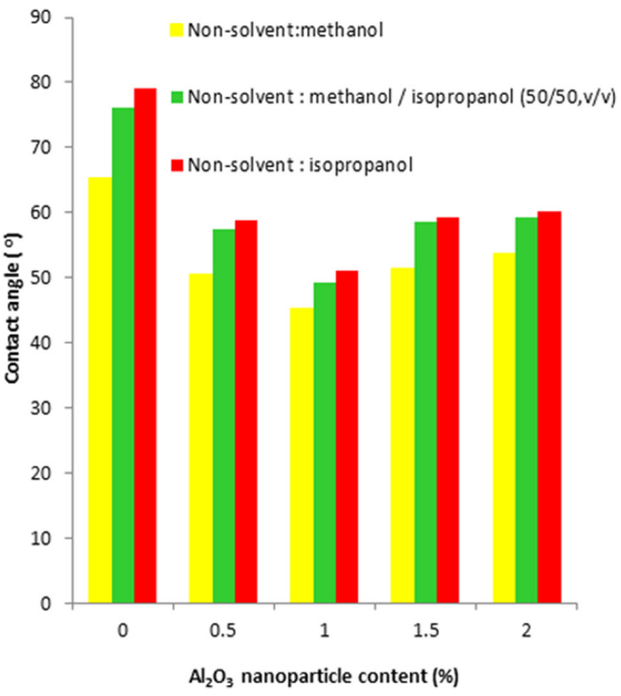

Fig. 10. Contact angle of the prepared membranes.

3.6. Filtration performance

3.6.1. Effect of Al_2O_3 nanoparticles concentration and non-solvent on pure water permeability

The membranes are subjected to pure water permeability for assessing their functions and operational evaluations. The adjusted operating condition is 7 bar and 25°C for transmembrane pressure and temperature, respectively. Fig. 11 reveals the effect of Al_2O_3 nanoparticle concentrations and non-solvents used in coagulation bath on pure water permeability of the prepared membranes. As shown, the prepared membranes with addition of Al_2O_3 nanoparticles present higher pure water permeability in comparison with the neat PBS membrane. At constant concentration of Al_2O_3 nanoparticles, the change of non-solvent from methanol to isopropanol reduces mutual diffusivities between components in the system during solidification of the casting solution. The precipitation process takes place slower which results in thinner membrane with low porosity. Thus, the membranes prepared at isopropanol have the lowest fluxes. As can be seen, initially, the pure water permeability of all membranes increases with the increase of Al_2O_3 nanoparticles concentration (up to 1 wt. %) and then slightly decreases due to the nanoparticle's coalesce. In fact, the membranes with higher porosity and thinner dense top layer presented higher pure water permeability. It is evident that there is a direct relationship between the porosity and permeability. As can be seen, pure water permeability for prepared membranes in methanol coagulation bath is located within the range of permeability for ultrafiltration membranes (10–50 $Lm^{-2}h^{-1}$ bar^{-1}) [41]. So these membranes act as UF (ultrafiltration) membranes.

According to Fig. 11, pure water permeability for prepared membranes in isopropanol and methanol/isopropanol (50/50, v/v) is less than 20 $Lm^{-2}h^{-1}$ bar^{-1}, therefore these membranes can act as NF (nanofiltration) membranes.

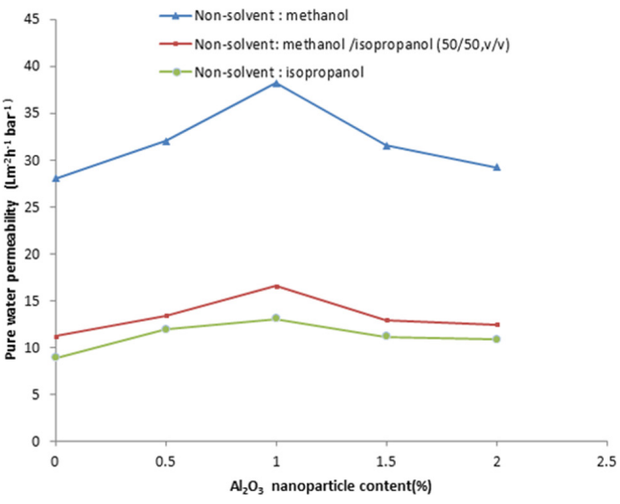

Fig. 11. Effect of Al_2O_3 nanoparticles concentration and non-solvent on pure water permeability.

3.6.2. Effect of Al_2O_3 nanoparticles concentration and non-solvent on permeation flux and rejection of membranes

Applying the same operating conditions (TMP = 7 bar and T = 25°C), the influences of the Al_2O_3 nanoparticle concentrations and also non-solvents on the permeation flux and rejection of wastewater pollution indices are respectively shown in Figs. 12 and 13. Obviously, the permeation flux increases with the introduction of nanoparticles. As can be seen in Fig. 12, the permeate flux of all membranes reduces

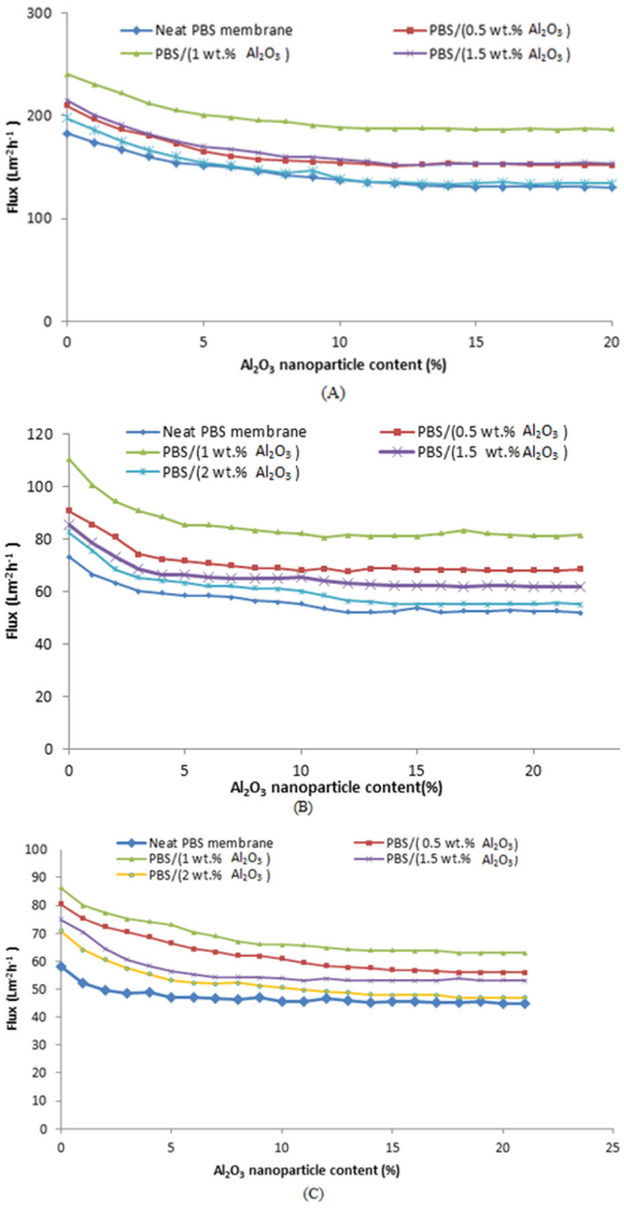

Fig. 12. Permeate flux of tomato canning wastewater through the membranes prepared at A) Methanol coagulation bath, B) Methanol/Isopropanol (50/50, v/v) coagulation bath and C) Isopropanol coagulation bath.

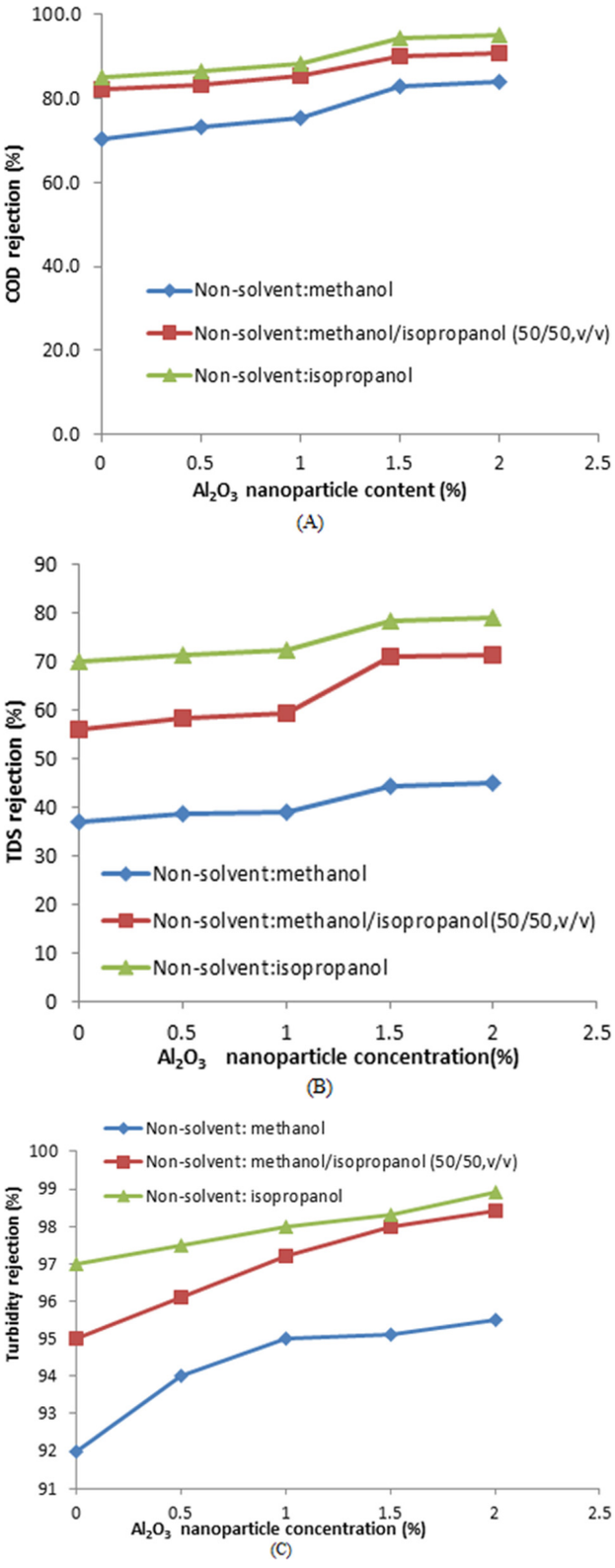

Fig. 13. Effect of Al_2O_3 nanoparticle concentration and non-solvent on rejection of membranes A) COD rejection, B) TDS rejection, C) Turbidity rejection.

drastically with time, which is rapid during the first 5 min and then follow by a more gradual decline until become constant. This behavior refers to concentration polarization and fouling of the membranes [3]. The trend of the waste water permeation flux is almost similar to that of pure water flux. So, the prepared membranes in isopropanol coagulation bath have lower fluxes than others. The weakened coagulation ability of isopropanol slows the precipitation rate during the immersion process, resulting in a thinner membrane (as shown in Fig. 7) which increases the formation of dense structure. In this case, less wastewater permeation is obtainable.

As shown all the prepared PBS/Al_2O_3 nanoparticle membranes in three non-solvents reveal higher rejection in comparison with the neat PBS membrane. The initial increase in Al_2O_3 nanoparticle concentrations up to 1 wt.% results in increasing the COD rejection. However, further increase in Al_2O_3 nanoparticles concentration up to 2 wt.%, results in smooth increasing (almost constant) the COD rejection of waste water. Increasing Al_2O_3 nanoparticles concentration in the polymer mixture enhances the retentions of COD in all membranes. Despite the flux increasing, this enhancement can be attributed to surface properties of the membranes which are changing by nanoparticle entrapment. The surface of Al_2O_3 entrapped membrane can be more hydrophilic than the neat polymeric membrane due to the higher affinity of metal oxides to water. Therefore, hydrophobic adsorption between sludge particle and Al_2O_3 entrapped membrane is reduced. As mentioned before, further increase in the Al_2O_3 nanoparticles concentration from 1 wt.% to 2 wt.%, results in the formation of denser structure and according to the above description, slightly increases the rejection value. According to Fig. 13(A), it is clear that maximum COD rejection is obtained by prepared membranes in isopropanol coagulation bath. It means that at constant concentration of Al_2O_3 nanoparticles, the change of non-solvent from methanol to isopropanol results in the formation of low porous structures which consequently increases the resistance against the transmission of waste water. Obviously with increasing porosity while increasing flux, the selectivity of membranes reduces. Therefore, membranes prepared in methanol coagulation bath with the most flux in comparison with others have less selectivity than other membranes and have not been able on the rejection of wastewater pollution indices. The results demonstrate that maximum COD rejection is obtained at the transmembrane pressure of 7 bars for prepared membrane in isopropanol coagulation bath with Al_2O_3 nanoparticles concentration of 1 wt.%.

With respect to Fig. 13B, the trend of TDS rejection is almost similar to that of COD rejection. The results reveal that membranes are prepared in methanol coagulation bath cannot be solely sufficient to reduce TDS of the wastewater. Meanwhile, membranes are prepared in isopropanol coagulation bath have better acted to remove of TDS.

Turbidity of wastewater using prepared membranes is well reduced. As shown in Fig. 13C, in the presence or absence of Al_2O_3 nanoparticles, turbidity rejection is above 92%. Therefore, adding the nanoparticles and using different non-solvents do not have a considerable effect on turbidity removal. As a result, among the synthesized membranes, PBS/Al_2O_3 nanoparticles 1 wt.% membrane that is prepared in isopropanol coagulation bath shows the remarkable performance as rejected turbidity, TDS and COD by 98.9, 79 and 94.9%, respectively.

Table 2.
Hydraulic resistance (R_m) of the membranes

Membranes prepared in methanol coagulation bath					
	Neat PBS	PBS/0.5 wt.% Al_2O_3	PBS/1 wt.% Al_2O_3	PBS/1.5 wt.% Al_2O_3	PBS/2 wt.% Al_2O_3
R_m(× 10^{14} m^{-1})	0.14	0.11	0.09	0.125	0.129
Membranes prepared in methanol/isopropanol (50/50,v/v) coagulation bath					
	Neat PBS	PBS/0.5 wt.% Al_2O_3	PBS/1 wt.% Al_2O_3	PBS/1.5 wt.% Al_2O_3	PBS/2 wt.% Al_2O_3
R_m(× 10^{14} m^{-1})	0.33	0.27	0.22	0.29	0.31
Membranes prepared in isopropanol coagulation bath					
	Neat PBS	PBS/0.5 wt.% Al_2O_3	PBS/1 wt.% Al_2O_3	PBS/1.5 wt.% Al_2O_3	PBS/2 wt.% Al_2O_3
R_m(× 10^{14} m^{-1})	0.44	0.41	0.36	0.37	0.39

3.7. Hydraulic resistance (R_m) of membranes

Hydraulic resistance (R_m) is determined from the inverse of line's slop that drawn through the pure water flux versus transmembrane pressure of (2 to 7 bars) data and is represented in Table 2. It is observed that the hydraulic resistance (R_m) of prepared membranes in isopropanol coagulation bath is higher compared to other membranes, which confirms that these membranes are low porous than the prepared membranes in methanol coagulation bath. The hydraulic resistance values of prepared PBS/Al_2O_3 nanoparticles 1 wt.% membranes in different coagulation baths are at the lowest. This result is in agreement with that of pure water flux experiments.

4. Conclusion

Modification of poly (1,4-butylene succinate) (PBS) membranes were carried out by the addition of different values of Al_2O_3 nanoparticles to the casting solution. These membranes were synthesized using the phase inversion process at different coagulation baths. The effect of Al_2O_3 nanoparticle concentration and non-solvent were evaluated on the membrane specifications including morphology, tensile strength, thermal stability, contact angle and treatment ability. The membrane morphology prepared in the methanol coagulation bath has presented higher porosity compared to membranes prepared in the methanol/isopropanol (50/50, v/v) and isopropanol coagulation baths. PBS membrane hydrophilicity was changed by the addition of Al_2O_3 nanoparticles to the casting solution, with porosity increasing (up to 1 wt.%) and the hydrophobic interaction between the membrane surface and foulants is decreasing. It was revealed that the tensile strength and modulus of the PBS/Al_2O_3 nanoparticles blended samples increase with increasing the Al_2O_3 nanoparticles content whereas their elongation-at-break showed an opposite tendency with further addition of nanoparticles(more than 1 wt.%).This behavior was attributed to the reinforcing effect of the Al_2O_3 nanoparticles that had been distributed in the PBS matrix and the brittleness of Al_2O_3 nanoparticles in comparison with the flexibility of polymer chains, respectively. To the thermal stability, the introduction of Al_2O_3 nanoparticles enhanced the thermal stabilization of the membrane. The membranes contact angle was reduced by addition of Al_2O_3 nanoparticles from 0 wt.% to 1 wt.%. Results showed that membranes were prepared in methanol coagulation bath have relatively low contact angles due to more porosity than others. Wastewater treatment and also permeation through the prepared membranes were noticeably affected by the Al_2O_3 nanoparticles content and non-solvent according to their direct effect on the membrane structure and surface porosity. Comparing the membranes abilities in reduction of wastewater pollution indices, prepared PBS/1 wt.% Al_2O_3 nanoparticles membrane in isopropanol coagulation bath was found to have the highest performance.

References

[1] L. Song, Z. Qiu, Crystallization behavior and thermal property of biodegradable poly(butylene succinate)/functional multi-walled carbon nanotubes nanocomposite, Polym. Degrad. Stab., 94 (2009) 632–637.
[2] Y.F. Shih, L.S. Chen, R.J. Jeng, Preparation and properties of biodegradable PBS/multi-walled carbon nanotube nanocomposites, Polymer, 49 (2008) 4602–4611.
[3] V. Ghaffarian, S.M. Mousavi, M. Bahreini, M. Afifi, Preparation and characterization of biodegradable blend membranes of PBS/CA, J. Polym. Environ., 21 (2013) 1150–1157.
[4] Q. Yang, M.i. Hirata, Y.I. Hsu, D. Lu, Y. Kimura, Improved thermal and mechanical properties of poly(butylene succinate) by polymer blending with a thermotropic liquid crystalline polyester, J. Appl. Polym. Sci., 131 (2014) n/a.
[5] W. Zhou, T. Xu, X. Wang, E. Zhi, J. Liu, W. Zhang, J. Ji, In situ polymerized nanocomposites of poly(butylene succinate)/TiO_2 nanofibers: molecular weight, morphology, and thermal properties, J. Appl. Polym. Sci., 127 (2013) 733–739.
[6] S. Sahoo, M. Misra, A.K. Mohanty, Biocomposites from switchgrass and lignin hybrid and poly(butylene succinate) bioplastic: studies on reactive compatibilization and performance evaluation, Macromol. Mater. Eng., 299 (2014) 178–189.
[7] H. Han, X. Wang, D. Wu, Mechanical properties, morphology and crystallization kinetic studies of bio-based thermoplastic composites of poly(butylene succinate) with recycled carbon fiber, J. Chem. Technol. Biotechnol., 88 (2013) 1200–1211.
[8] J. Zhan, Y. Chen, G. Tang, H. Pan, Q. Zhang, L. Song, Y. Hu, Crystallization and melting properties of poly(butylene succinate) composites with titanium dioxide nanotubes or hydroxyapatite nanorods, J. Appl. Polym. Sci., 131 (2014) n/a.
[9] J. Xu, B.H. Guo, Poly(butylene succinate) and its copolymers: Research, development and industrialization, Biotechnol. J., 5 (2010) 1149–1163.

[10] E. Zakharova, C. Lavilla, A. Alla, A. Martínez de Ilarduya, S. Muñoz-Guerra, Modification of properties of poly(butylene succinate) by copolymerization with tartaric acid-based monomers, Eur. Polym. J., 61 (2014) 263–273.
[11] S.S. Park, S.H. Chae, S.S. Im, Transesterification and crystallization behavior of poly(butylene succinate)/poly(butylene terephthalate) block copolymers, J. Polym. Sci., Part A: Polym. Chem., 36 (1998) 147–156.
[12] H.L. Richards, P.G.L. Baker, E. Iwuoha, Metal nanoparticle modified polysulfone membranes for use in wastewater treatment: A Critical Review, J. SEMAT, 2 (2012) 183–193.
[13] S.S. Ray, M. Bousmina, Biodegradable polymers and their layered silicate nanocomposites: In greening the 21st century materials world, Prog. Mater. Sci., 50 (2005) 962–1079.
[14] W. Guo, Y. Zhang, W. Zhang, Mechanical properties and crystallization behavior of hydroxyapatite/poly(butylenes succinate) composites, J. Biomed. Mater. Res., 101 (2013) 2500–2506.
[15] B.P. Calabia, F. Ninomiya, H. Yagi, A. Oishi, K. Taguchi, M. Kunioka, M. Funabashi, Biodegradable poly(butylene succinate) composites reinforced by cotton fiber with silane coupling agent, Polymers, 5 (2013) 128–141.
[16] S. Zhu, Y. Zhao, Z. Qiu, Biodegradable poly (butylene succinate-co-butylene adipate)/multiwalled carbon nanotube nanocomposites: preparation, morphology, and crystallization behavior, J. Appl. Polym. Sci., 124 (2012) 4268–4273.
[17] N. Jacquel, R. Saint-Loup, J.P. Pascault, A. Rousseau, F. Fenouillot, Structure-properties relationship of in situ synthesized poly(butylene succinate)/silica nanocomposites: application in extrusion blowing of films, Macromol. Mater. Eng., 299 (2014) 977–989.
[18] K. Hong, K. Nakayama, S. Park, Effects of protective colloids on the preparation poly(l-Lactide)/poly(butylene succinate) microcapsules, Eur. Polym. J., 38 (2002) 305–311.
[19] L.Y. Ng, A.W. Mohammad, C.P. Leo, N. Hilal, Polymeric membranes incorporated with metal/metal oxide nanoparticles: A comprehensive review, Desalination, 308 (2013) 15–33.
[20] T. Tanaka, T. Tsuchiya, H. Takahashi, M. Taniguchi, D.R. Lloyd, Microfiltration membrane of polymer blend of poly(L-lactic acid) and poly(ε-caprolactone), Desalination, 193 (2006) 367–374.
[21] S.S. Silva, M.I. Santos, O.P. Coutinho, J.F. Mano, R.L. Reis, Physical properties and biocompatibility of chitosan/soy blended membranes, J. Mater. Sci. - Mater. Med., 16 (2005) 575–579.
[22] K. Uto, K. Yamamoto, S. Hirase, T. Aoyagi, Temperature-responsive cross-linked poly(ε-caprolactone) membrane that functions near body temperature, J. Control. Rel., 110 (2006) 408–413.
[23] J.W. Chena, K.F. Tseng, S. Delimartin, C.K. Lee, M.H. Ho, Preparation of biocompatible membranes by electrospinning, Desalination, 233 (2008) 48–54.
[24] A. Moriya, P. Shen, Y. Ohmukai, T. Maruyama, H. Matsuyama, Reduction of fouling on poly(lactic acid) hollow fiber membranes by blending with poly(lactic acid)–polyethylene glycol–poly(lactic acid) triblock copolymers, J. Membr. Sci., 415–416 (2012) 712–717.
[25] V. Ghaffarian, S.M. Mousavi, M. Bahreini, H. Jalaei, Polyethersulfone/poly (butylene succinate) membrane: Effect of preparation conditions on properties and performance, J. Ind. Eng. Chem., 20 (2014) 1359–1366.
[26] N. Maximous, G. Nakhla, W. Wan, K. Wong, Preparation characterization and performance of Al_2O_3/PES membrane for wastewater filtration, J. Membr. Sci., 341 (2009) 67–75.
[27] P. Sukitpaneenit, T.S. Chung, Molecular elucidation of morphology and mechanical properties of PVDF hollow fiber membranes from aspects of phase inversion, crystallization and rheology, J. Membr. Sci., 340 (2009) 192–205.
[28] T. Tanaka, M. Takahashi, S. Kawaguchi, T. Hashimoto, H. Saitoh, T. Kouya, M. Taniguchi, D.R. Lloyd, Formation of microporous membranes of poly(1,4-butylene succinate) via nonsolvent and thermally induced phase separation, Desal. Water Treat., 17 (2010) 176–182.
[29] J.N. Shena, H.M. Ruana, L.G. Wub, C.J. Gaoc, Preparation and characterization of PES–SiO_2 organic–inorganic composite ultrafiltration membrane for raw water pretreatment, Chem. Eng. J., 168 (2011) 1272–1278.
[30] B.S. Lalia, V. Kochkodan, R. Hashaikeh, N. Hilal, A review on membrane fabrication: Structure, properties and performance relationship, Desalination, 326 (2013) 77–95.
[31] P. van de Witte, p.j. Dijkstra, J.W.A. van den Berg, J. Feijen, Phase separation processes in polymer solutions in relation to membrane formation, J. Membr. Sci., 117 (1996) 1–31.
[32] J.H. Li, Y.Y. Xu, L.P. Zhu, J.H. Wang, C.H. Du, Fabrication and characterization of a novel TiO_2 nanoparticle self-assembly membrane with improved fouling resistance, J. Membr. Sci., 326 (2009) 659–666.
[33] F. Shen, X. Lu, X. Bian, L. Shi, Preparation and hydrophilicity study of poly(vinyl butyral)-based ultrafiltration membranes, J. Membr. Sci., 265 (2005) 74–84.
[34] M.B. Thürmera, P. Polettob, M. Marcolinb, J. Duarteb, M. Zeni, Effect of non-solvents used in the coagulation bath on morphology of PVDF membranes, Mat. Res., 15 (2012) 884–890.
[35] E. Drioli, L. Giorno, Comprehensive membrane science and engineering, Elsevier, 2010.
[36] I.C. Kim, K.H. Lee, T.M. Tak, Preparation and characterization of integrally skinned uncharged polyetherimide asymmetric nanofiltration membrane, J. Membr. Sci., 183 (2001) 235–247.
[37] G.B. Appetecchi, F. Croce, P. Romagnoli, B. Scrosati, U. Heider, R. Oesten, High-performance gel-type lithium electrolyte membranes, Electrochem Commun., 1 (1999) 83–86.
[38] A. Samimi, S.A. Mousavi, A. Moallemzadeh, R. Roostaazad, M. Hesampour, A. Pihlajamäki, M. Mänttäri, Preparation and characterization of PES and PSU membrane humidifiers, J. Membr. Sci., 383 (2011) 197–205.
[39] G. Wu, S. Gan, L. Cui, Y. Xu, Preparation and characterization of PES/TiO_2 composite membranes, Appl. Surf. Sci., 254 (2008) 7080–7086.
[40] L. Yan, Y.S. Li, C.B. Xiang, S. Xianda, Effect of nano-sized Al_2O_3-particle addition on PVDF ultrafiltration membrane performance, J. Membr. Sci., 276 (2006) 162–167.
[41] R.W. Baker, Membrane technologhy and applications, John Wiley & Sons, 2004.